Clays and Clay Minerals, Vol. 38, No. 1, 97–108, 1990.

MINERAL ASSEMBLAGES OF VOLCANIC AND DETRITAL PARTINGS IN TERTIARY COAL BEDS, KENAI PENINSULA, ALASKA

LINDA M. REININK-SMITH

Mineral Industry Research Laboratory, University of Alaska Fairbanks
Fairbanks, Alaska 99775

Abstract—Volcanic and non-volcanic partings are exposed in coal beds of the Tertiary Beluga and Sterling Formations along the shores of the Kenai lowland, Alaska. About two-thirds of the partings originated as air-fall tephra which fell in coal-forming swamps. The tephra partings in the Pliocene strata are unaltered or slightly altered and have a characteristic mineral assemblage of volcanic glass ± montmorillonite ± kaolinite ± opal-CT. Miocene strata are slightly altered to totally altered, and a typical mineral assemblage consists of feldspar ± kaolinite ± montmorillonite ± quartz ± crandallite ± altered volcanic glass. Crandallite appears to have formed early in diagenesis by the replacement of volcanic glass prior to the formation of montmorillonite and kaolinite.

About one-third of the partings originated primarily as detrital sediments derived from surrounding metamorphic and sedimentary terranes and were deposited by periodic floods. Mixtures of tephra and detrital sediments were also noted and were difficult to distinguish from tephra partings in the field. Detrital partings are characterized by detrital chlorite + illite + smectite + quartz ± feldspar ± siderite ± kaolinite. The chlorite in these strata is allogenic. Smectite is less common in the detrital partings.

Key Words—Chlorite, Coal partings, Crandallite, Illite, Kaolinite, Opal-CT, Smectite, Volcanic ash.

INTRODUCTION

Tertiary coal beds are exposed along the shores and coastal canyons of the Kenai lowland on the Kenai Peninsula of the Cook Inlet area, Alaska. The coal formed in a series of swamps in poorly drained flood basins associated with meandering- and braided-stream sedimentation (Hayes *et al.*, 1976; Rawlinson, 1979). Four sedimentary units, the Kenai Group, were deposited during Neogene time (Figure 1). This study focuses on two of these units, the Beluga and the Sterling Formations. The outcrops were described by Barnes and Cobb (1959) and were subdivided into the Homerian and the Clamgulchian provincial paleobotanical stages by Wolfe *et al.* (1966). The boundary between the stages, which approximates the lithostratigraphic boundary between the Beluga and Sterling Formations, was assigned an age of 7.9 ± 1.0 m.y.b.p. based on K-Ar age estimates for plagioclase and fission-tracks in zircon from tephra interbedded in coal (Triplehorn *et al.*, 1977).

Volcanic activity was common in the Cook Inlet area during the middle and late Tertiary, related to underthrusting along the Aleutian Trench and subsequent uplift of the Alaska Range and the Kenai-Chugach Mountains (Kirshner and Lyon, 1973). Layers of air-fall tephra and fluvial clastic sediments were incorporated into the coal swamps and are now exposed as partings in the coal beds. These partings have not been previously systematically characterized. It is important to do so because the tephra partings can be used for correlation of the Kenai lowland strata (to be reported elsewhere), for estimating coal resources, and for potential correlation with the subsurface of the Cook Inlet. In addition, the frequency of past volcanism in the Cook Inlet area can be interpreted by careful documentation of tephra partings in the coal beds (also to be reported elsewhere). The purpose of this study is (1) to demonstrate that tephra and detrital partings can be differentiated on the basis of their clay and whole-rock mineral assemblages, (2) to investigate whether Miocene and Pliocene sections differ in mineral compositions, and (3) to describe a new occurrence of crandallite.

SAMPLE SITES AND SAMPLE SELECTION

About 100 partings, 1–10-cm thick, were sampled. Partings <5 cm were sampled only if partings were rare or if they displayed unusual properties. Sixty-two samples were obtained from the Diamond Creek (DC) section of the Beluga Formation and 35 samples (three from siltstone) from the McNeil Canyon (MC), Fox Creek (FC), Ninilchik (NIN), and Clam Gulch (CG) sections of the Sterling Formation. "Section" here signifies continuously sampled outcrops (Figure 2) and does not necessarily coincide with the measured sections described by Barnes and Cobb (1959), Adkison *et al.* (1975), Rawlinson (1979), or Merritt *et al.* (1987). Partings are especially well-preserved in the DC section, which contains by far more individual coal beds and thus more partings than younger sections.

ANALYTICAL METHODS

More than 500 whole rock and <2-μm-size fractions were analyzed using a Rigaku X-ray diffractometer and Ni-filtered CuKα radiation at a scanning rate of 8°2θ/min. To test the accuracy of the X-ray powder diffraction (XRD) scans ob-

Copyright © 1990, The Clay Minerals Society

https://doi.org/10.1346/CCMN.1990.0380113 Published online by Cambridge University Press

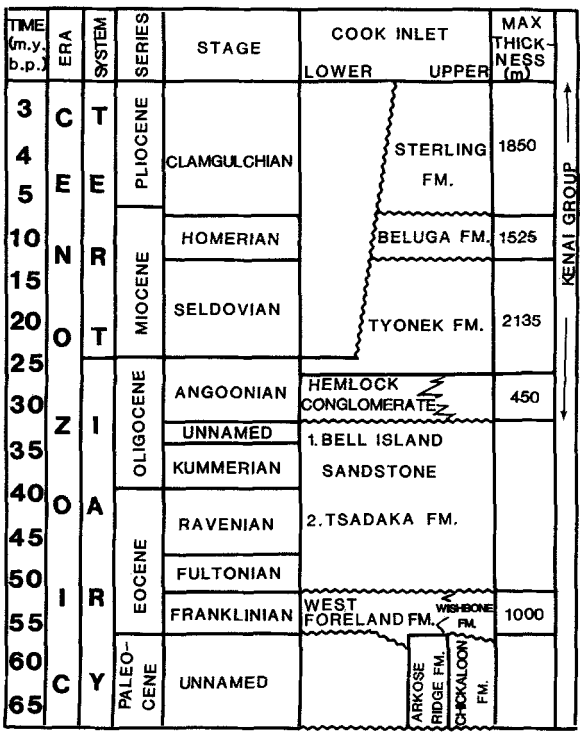

Figure 1. Stratigraphic column of the Cook Inlet Tertiary formations. Modified from Fisher and Magoon (1979).

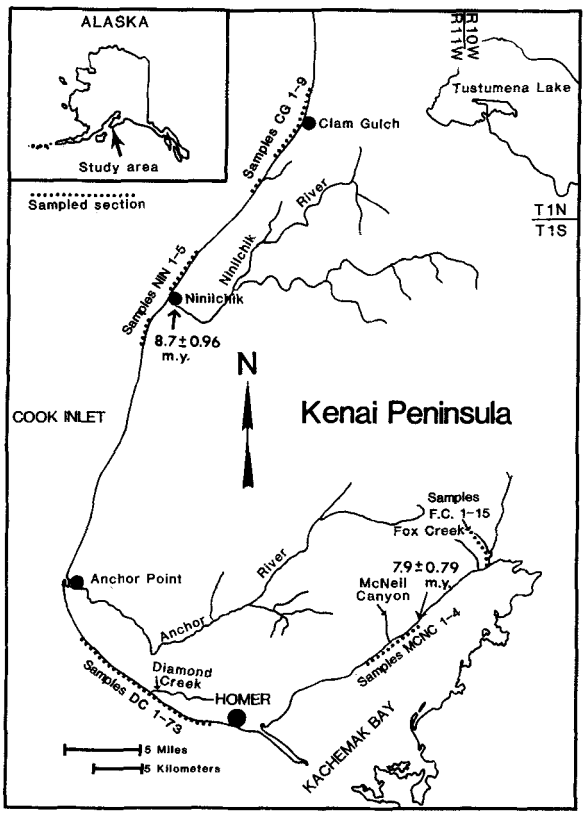

Figure 2. Index map showing the location of the study area. Sampled sections are shown as lines of continuous dots. K-Ar radiometric ages of plagioclase near Ninilchik and McNeil Canyon are from Triplehorn *et al.* (1977). FC = Fox Creek, MC = McNeil Canyon, DC = Diamond Creek, NIN = Ninilchik, CG = Clam Gulch.

tained at this speed, 20 air-dried clay samples and 5 powdered bulk samples were also X-rayed at both 2° and 1°2θ/min. The peaks were only insignificantly less defined at 8°2θ/min, as shown in Figure 3. Peak intensity and sharpness were not affected for any sample. Only qualitative comparisons of mineral content were required for this study.

Whole-rock sample preparation

Whole rock samples were ground to a <200 mesh powder, pressed into aluminum sample holders and X-rayed (2° to 65°2θ). Small chips of whole-rock samples were selected on the basis of mineral content as determined by XRD powder diffraction, mounted on aluminum stubs, and sputter-coated with a gold-palladium alloy. These samples were analyzed using a JEOL (JSM35 model) scanning electron microscope (SEM) at 15 kV and a KEVEX Unispec System 7000 energy-dispersive X-ray spectrometer (EDX).

Seven indurated tephra samples were made into thin sections. An ultrasonic probe was used to disaggregate the coarse fractions (~0.08 to 1.0 mm) from 16 water-immersed, crumbly samples, which were subsequently thin-sectioned as petrographic grain mounts.

A Perkin-Elmer 283B infrared (IR) spectrophotometer was used according to the methods of Van der Marel and Beutelspacher (1976) to determine whether small amounts of kaolinite were present in chlorite-rich, detrital samples. A direct-current plasma (DCP), atomic emission spectrometer (Beckman SpectraSpan V) was used to determine the major elements in all samples.

Clay-fraction sample preparation

Each sample was disaggregated with an ultrasonic probe and centrifuged at 1000 rpm for 4 min. The time and speed, after methods of Jackson (1974), left only the <2-μm-size fraction in suspension which was suction-deposited on a porous, unglazed ceramic plate, as described by Kinter and Diamond (1956). Each sample was scanned from 2° to 35°2θ after air drying, from 2° to 20°2θ after vapor-phase ethylene glycolation for one week, and after step-wise heating to 300° and 550°C, respectively, for 1 hr or longer. To determine whether montmorillonite or beidellite was present, eight of the purest smectite samples were air-dried, saturated with 2 N LiCl, heated at 250°C for 12 hr, and solvated with ethylene glycol and glycerol according to the test devised by Greene-Kelly (1955).

RESULTS

Outcrop distinctions

Tephra partings were clayey, plastic, indurated or crumbly, had a homogenous texture, and were as much as 10 cm thick. They commonly were more coarse-grained than the detrital partings and weathered to a bleached, pinkish white color on surface exposures. Pumice fragments were visible in some indurated partings, but also occurred as dispersed pumice partings. Colors were commonly 10R6/3 pale red to 10R2.5/2

https://doi.org/10.1346/CCMN.1990.0380113 Published online by Cambridge University Press

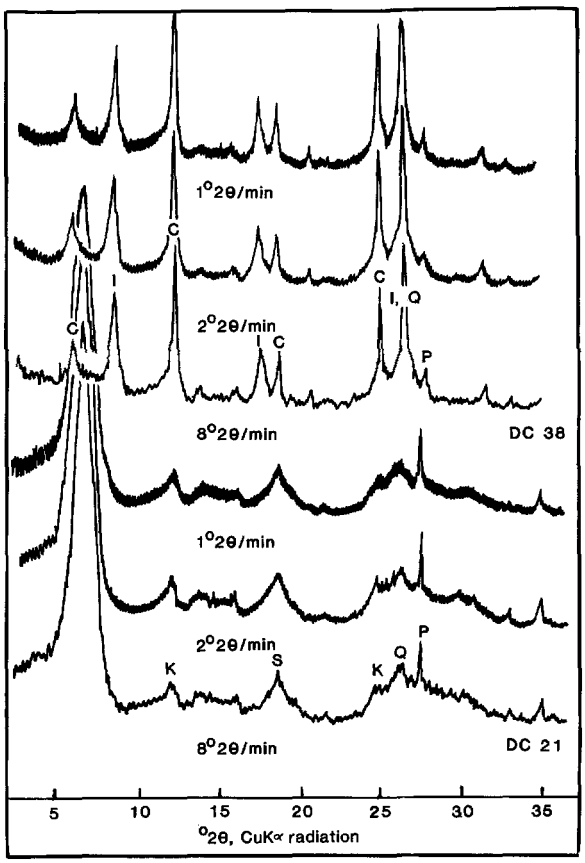

Figure 3. Comparison of X-ray powder diffraction patterns of two <2-μm, air-dried samples at three scan rates: 8°2θ/min (chart speed: 80 mm/min), 2°2θ/min (chart speed: 20 mm/min), and 1°2θ/min (chart speed: 10 mm/min).

very dusky red (Munsell Soil Color Charts). Organic materials showed no preferred orientation.

Detrital partings tended to be flaky, fissile, or crumbly and were only locally indurated. They were finer grained, thicker, and had a more heterogenous texture than most volcanic partings. If weathered, they commonly retained their original color or developed a faded appearance. They were commonly 10YR7/1 light gray to 10YR3/1 very dark gray and locally had blue or green tinges. Organic materials were oriented parallel to the fissility—probably the bedding plane. Pumice fragments or other products of volcanic activity were not observed.

Tephra partings

Whole-rock mineralogy. The 001 smectite reflections in the XRD patterns were poorly developed. The 060 reflections ranged from 1.49 to 1.50 Å, indicating dioctahedral smectite. Kaolinite was present only as weak peaks in patterns of the randomly oriented whole-rock samples.

At least 15 partings in the lower part of the DC

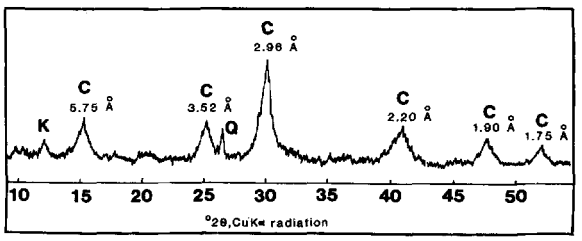

Figure 4. X-ray powder diffraction pattern of sample DC 60a. C = crandallite, Q = quartz and K = kaolinite.

section (identical to measured section 1b of Adkison *et al.*, 1975) contained minerals of the crandallite group. The general formula of this solid solution series is $XAl_3(PO_4)_2(OH)_5 \cdot H_2O$, where X may be Sr (goyazite), Ba (gorceixite), or Ca (crandallite) (Fleisher *et al.*, 1984). Specific crandallite-group minerals are difficult to identify by XRD or SEM because of the solid solution compositional variations and a general lack of features that distinguish different members of this group. Elemental analyses (Table 1) and EDX data for the DC samples, however, showed that Ca > Ba > Sr; thus the mineral was compositionally crandallite. Crandallite was identified from the whole rock XRD patterns by reflection maxima at 2.96 Å (Figure 4). EDX suggested that the crandallite was present in some samples in amounts too small for XRD detection. SEMs show nodular, bulbous, commonly hollow structures (Figure 5).

Values of P_2O_5, BaO, and SrO greater than any yet reported from Tertiary Alaskan coal sequences were obtained for the DC samples. For example, the P_2O_5 content of sample DC 60A was 28.79% (Table 1), which compares with a maximum of 17.1% P_2O_5 in coal ash from the Chuitna River coal (Rao and Smith, 1987). XRD patterns and chemical analyses of 35 samples from the MC, FC, NIN, and CG sections, however, failed to reveal crandallite or elevated concentrations of Ca, Ba, Sr, or P (Table 2).

Opal-CT was identified as a trace constituent in three samples (FC 8, NIN 4, and CG 5). Weak, broad peaks at 4.05 Å were recognized in the XRD patterns of samples FC 8 and CG 5, which contained little or no feldspar that could have interfered with the identification. No other opal-CT peaks were noted in these samples. In sample NIN 4 the intensity of the 4.04-Å feldspar peak was anomalously strong, and small opal-CT peaks at 3.13 and 2.49 Å were noted.

Quartz was identified in 45 of the 68 partings, typically in small amounts. Volcanic quartz was also observed in thin sections of the coarse fractions. Most of it, was unaltered, but some showed straight extinction, β-quartz morphology, subhedral and angular shapes, and local embayments. In less altered samples, some angular quartz grains showed glassy fringes of volcanic origin.

https://doi.org/10.1346/CCMN.1990.0380113 Published online by Cambridge University Press

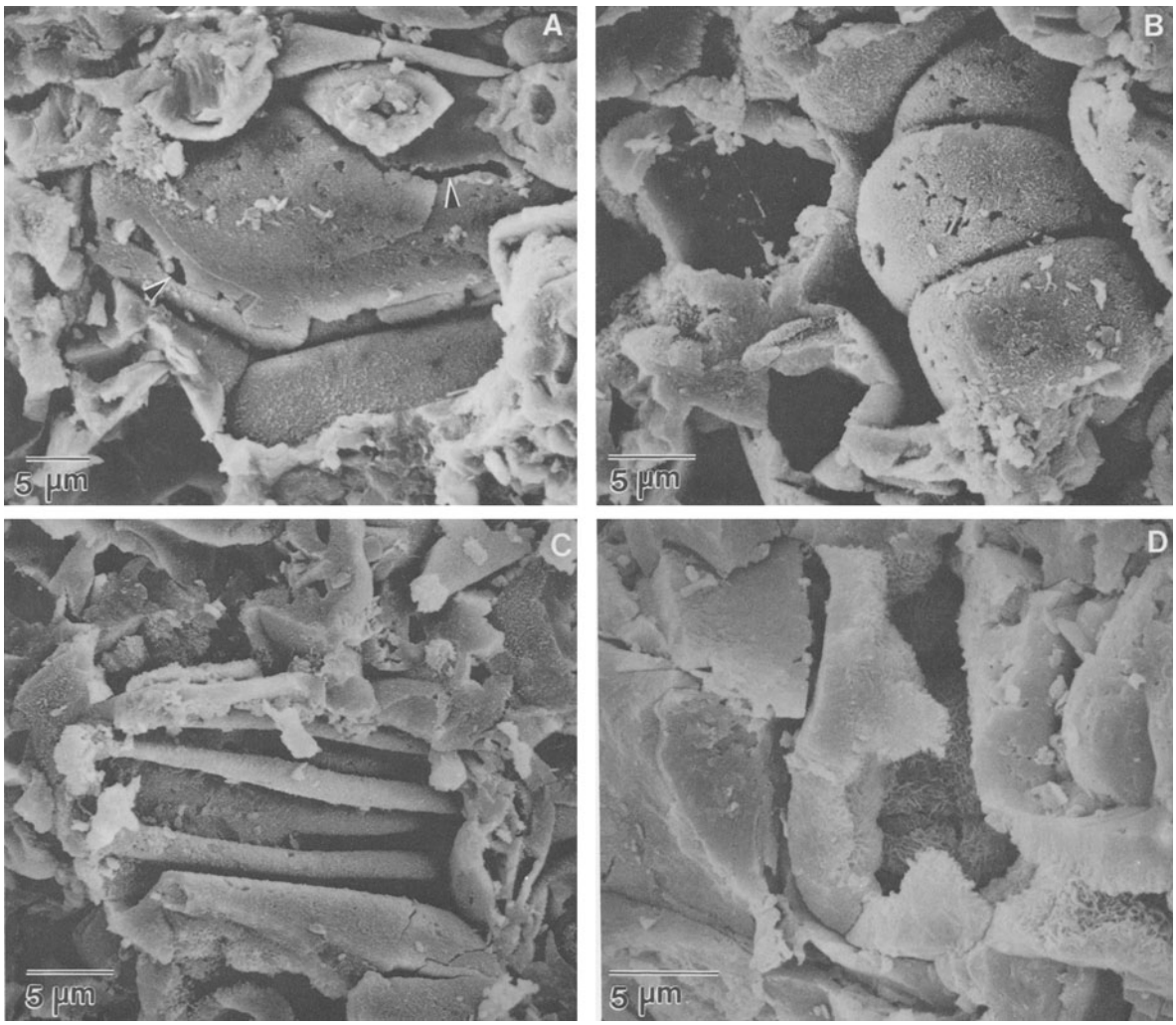

Figure 5. Scanning electron micrograph of crandallite-group minerals in samples DC 60 and DC 68: (A) straight-edged contacts of hollow structures, which may be crandallite-replaced, volcanic bubble-wall shards. Note holes on the surface (arrows) indicating the hollow interior (2200× = original magnification, sample DC 60A). (B) possible pseudomorphs of bubble-wall, hollow shards. Two of the "bubbles" on the left side of the photo appear to have had their tops sheared off, and the empty interiors are clearly visible (3000× = original magnification, sample DC 60A). (C) columnules (3000×, sample DC 60A). (D) smectite lining a cavity in grain having a crandallite-like composition (3600×, sample DC 68).

Feldspar was identified in 61 of the 68 tephra partings. In thin sections of the coarse fractions, plagioclase was much more abundant than K-feldspar and occurred as angular and euhedral crystals, indicating volcanic origin and minimal transportation. Trace amounts of sanidine were noted. Highly zoned plagioclase was common. SEM showed pitted and etched surfaces on some plagioclase grains and alteration to smectite on others. Three tephra partings contained mostly unaltered volcanic glass and a few feldspar grains, some of which displayed glass fringes.

Green hornblende, pyroxene, some polycrystalline quartz, volcanic rock fragments, titaniferous magnetite, traces of olivine, zircon, apatite, and biotite, and rare muscovite were also identified. The few muscovite grains were probably detrital. The presence of amphiboles was questionably indicated in some samples by very weak XRD peaks.

Clay mineralogy. Smectite was the dominant component in the clay fraction. Typical XRD patterns showed an intense, broad 001 peak at about 12–14 Å, which expanded in all samples to 17.0 Å with ethylene glycol solvation. Smectite from samples containing abundant, unaltered volcanic glass appeared to be poorly crystalline; weak and broad XRD peaks were present in the air-dried preparations, which expanded to prominent 17.0-Å peaks with ethylene glycol solvation. The LiCl test (Greene-Kelly, 1955), established the smectite from eight samples as montmorillonite; the 001 smec-

https://doi.org/10.1346/CCMN.1990.0380113 Published online by Cambridge University Press

Table 1. Major oxide analyses of crandallite-bearing partings from the Beluga Formation.[1]

	DC 1	DC 8	DC 12	DC 29	DC 40	DC 40a	DC 51	DC 51a	DC 53	DC 57	DC 58	DC 60	DC 60a	DC 69	DC 70	DC 71
SiO_2	23.23	46.29	36.70	52.47	42.93	43.85	16.48	39.55	40.41	41.92	54.98	33.73	7.16	36.87	17.94	40.72
Al_2O_3	34.67	30.36	30.34	31.60	33.76	33.00	40.57	34.72	30.36	29.67	24.30	28.83	39.62	29.98	34.28	31.13
Fe_2O_3[2]	1.66	2.28	1.19	2.22	0.97	1.02	0.41	0.70	0.94	1.46	3.48	1.39	0.48	0.62	2.03	1.12
MgO	0.67	2.03	1.03	1.84	1.58	1.75	0.20	<0.01	0.90	0.50	1.75	1.37	0.08	0.98	1.45	0.81
CaO	7.29	4.10	10.85	2.62	4.60	4.91	10.60	8.77	10.50	11.37	3.38	11.24	10.32	11.33	8.75	8.41
Na_2O	0.15	0.38	1.01	1.10	1.04	1.00	1.10	1.51	4.22	4.21	1.69	2.23	0.75	3.43	0.50	3.19
K_2O	1.98	0.33	0.18	0.38	0.17	0.13	0.17	0.21	0.32	0.12	1.91	0.31	0.11	0.19	0.59	1.15
TiO_2	1.79	2.41	0.81	2.08	0.60	0.61	0.46	0.68	0.66	0.56	0.95	2.16	0.96	0.69	2.52	0.98
MnO	0.03	0.01	0.01	0.01	<0.01	<0.01	<0.01	<0.01	0.04	0.02	0.04	0.01	<0.01	<0.01	0.03	0.01
P_2O_5	21.87	9.64	15.09	3.93	9.28	9.15	22.32	10.42	9.67	8.29	5.77	15.57	28.79	12.41	22.68	8.91
BaO	4.30	1.35	1.82	0.64	2.67	2.61	3.74	0.85	1.67	1.19	0.85	2.42	5.68	1.75	5.51	2.08
SrO	2.60	0.91	1.25	0.32	2.50	2.36	4.38	1.16	1.18	0.99	0.68	1.77	5.28	1.55	3.48	1.52
Total	100.24	100.09	100.27	99.21	100.10	100.39	100.43	98.57	100.87	100.29	99.78	101.02	99.23	99.79	99.76	100.03

[1] Values are calculated on a moisture-free basis. Each parting was analyzed in quadruplicate. Corrected value (on moisture-free basis) = $\frac{100}{100 - \text{L.O.I.}} \times$ oxide wt.%.

[2] Total Fe calculated as Fe_2O_3.

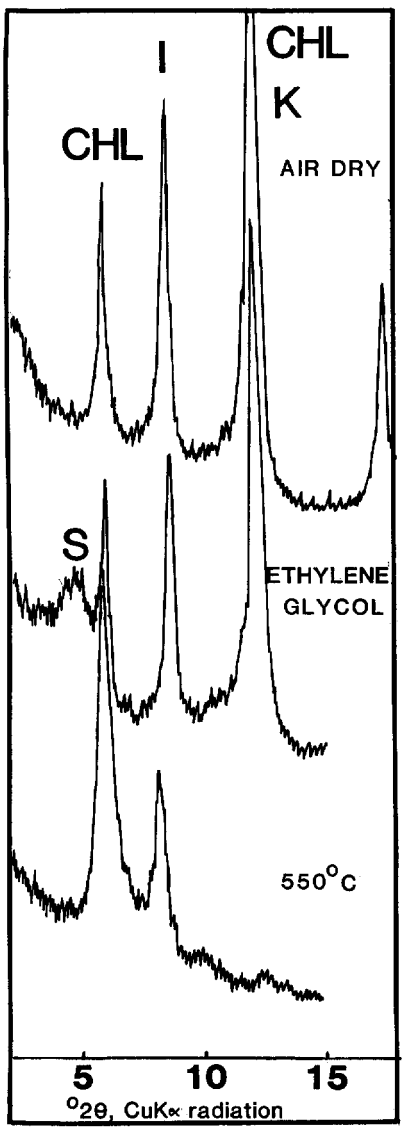

Figure 6. X-ray powder diffraction pattern of oriented clay sample from detrital parting (DC 4) showing sharp, prominent peaks typical of detrital chlorite and illite. CHL = chlorite, I = illite, S = smectite, K = kaolinite.

tite peaks did not shift after ethylene glycol and glycerol solvation, suggesting that the smectite in the other tephra partings was also montmorillonite.

Kaolinite was identified in most of the tephra partings in the DC section on the basis of a sharp reflection at 7.14 to 7.25 Å in oriented, <2-μm-size fractions. Kaolinite was a minor component or absent in partings from the younger sections.

Detrital partings

Whole-rock mineralogy. Siderite was detected in seven partings on the basis of sharp, prominent XRD peaks. Partings containing siderite were remarkably uniform,

https://doi.org/10.1346/CCMN.1990.0380113 Published online by Cambridge University Press

Table 2. Representative analyses of siderite-rich, detrital and altered tephra partings.[1]

	Siderite-rich partings						Detrital partings					
	DC 8b	DC 38	DC 48	DC 56	DC 67	CG 4	DC 4	DC 6	DC 17	DC 28	DC 30	NIN 5
SiO_2	20.99	53.21	24.17	25.19	40.96	31.14	62.47	60.17	59.87	59.89	58.13	63.61
Al_2O_3	7.23	19.67	7.00	11.60	15.39	8.67	20.02	20.87	23.84	19.35	21.35	18.68
Fe_2O_3[2]	61.19	18.26	55.69	51.68	36.16	49.95	8.95	8.56	6.78	11.89	10.05	6.89
MgO	2.22	2.43	3.86	2.23	2.29	1.98	2.58	2.73	2.28	2.39	2.57	2.46
CaO	2.48	0.88	4.35	1.39	0.99	2.85	0.51	0.79	0.80	0.90	0.68	1.84
Na_2O	1.22	1.10	1.25	1.16	1.12	2.42	1.22	1.00	1.18	1.50	1.11	3.12
K_2O	0.95	2.64	0.89	1.66	1.68	1.15	2.36	2.91	2.56	2.31	2.73	2.01
TiO_2	0.36	0.79	0.44	0.35	0.58	0.43	0.96	0.91	0.95	0.91	0.91	0.96
MnO	1.67	0.36	0.83	0.98	1.05	1.17	0.15	0.10	0.09	0.24	0.18	0.09
P_2O_5	0.17	0.19	0.62	0.32	0.13	0.31	0.07	0.10	0.11	0.16	0.05	0.12
BaO	0.05	0.11	0.18	0.18	0.06	0.05	0.16	0.11	0.10	0.09	0.18	0.09
SrO	0.01	0.01	0.12	0.12	<0.01	0.01	0.09	0.02	0.01	0.02	0.09	0.02
Total	98.54	99.65	99.40	96.86	100.40	100.13	98.53	98.28	98.57	99.65	98.03	99.88

	DC altered tephra partings						FC, MC, NIN, CG, tephra partings					
	DC 8a	DC 21	DC 40d	DC 54	DC 65	DC 68a	FC 6	FC 12	MC 3	MC 4	NIN 2	CG 6
SiO_2	62.76	62.58	60.23	61.48	61.21	59.19	69.56	72.29	60.28	66.06	63.17	70.98
Al_2O_3	23.04	25.06	25.48	24.66	23.57	30.34	16.29	17.44	23.41	20.67	21.27	15.96
Fe_2O_3[2]	2.98	2.12	1.76	2.00	2.26	1.33	3.82	1.58	3.63	2.73	2.01	2.17
MgO	2.23	2.45	2.18	2.20	2.20	1.47	1.07	0.54	1.58	1.30	0.50	0.78
CaO	3.49	3.70	5.27	4.47	5.94	3.39	2.25	2.88	5.72	4.05	5.39	2.14
Na_2O	3.47	1.30	1.61	2.79	3.90	3.28	2.90	1.44	3.50	3.24	5.30	3.80
K_2O	0.76	0.34	0.16	0.30	0.16	0.30	2.93	2.20	0.36	1.12	1.18	3.27
TiO_2	0.66	1.84	0.33	0.66	0.46	0.83	0.75	0.28	0.64	0.34	0.51	0.32
MnO	0.02	0.01	<0.01	0.05	0.01	<0.01	0.06	0.06	0.01	0.01	0.02	0.04
P_2O_5	0.35	0.15	0.59	0.40	0.38	0.02	0.14	0.11	0.44	0.17	0.06	0.09
BaO	0.08	0.08	0.19	0.07	0.10	0.01	0.12	0.17	0.09	0.08	0.04	0.09
SrO	0.05	0.05	0.16	0.10	0.09	0.03	0.03	0.14	0.09	0.10	0.11	0.04
Total	99.89	99.69	99.97	99.18	100.27	100.20	99.92	99.14	99.75	99.86	99.57	99.67

[1] Analyses were calculated on a moisture-free basis. Each sample was analyzed in quadruplicate. Corrected value (on moisture-free basis) $= \frac{100}{100 - \text{L.O.I.}} \times$ oxide wt.%.

[2] Total Fe calculated as Fe_2O_3.

coarse-grained, dark brown-gray to nearly black layers in the coal; one occurrence was in the form of concretions in a silty layer. Two of three partings collected from a single coal bed were indurated and coarse-grained, and one was flaky.

All 27 detrital partings contained mostly subequant quartz grains. The XRD peaks were high and sharp compared with the quartz peaks from the tephra partings. Twenty-four of the detrital partings contained feldspar. Most of the feldspar grains from the coarse fractions were rounded plagioclase having pitted and altered surfaces. Sanidine was not detected. Accessory components, such as shale, chert, metamorphic chlorite-rich rock fragments, muscovite, and traces of epidote, were detected in a few thin sections.

Clay mineralogy. Illite and minor smectite were identified in all detrital samples. The 001 reflections of illite were superimposed on the smectite (illite/smectite (?)) 001 peak in the XRD patterns of most air-dried samples. The intensity of the illite 10.2-Å peak decreased with ethylene glycol solvation, and a broad, weak peak at 17.0 Å appeared (Figure 6). At 300° and 550°C, the 17.0-Å peak collapsed to about 9.7 Å. K-saturation and heating to 400°C of five detrital samples also produced superimposed 001 reflections of smectite and illite, suggesting that the expandable component was smectite. Based on comparison with EDX spectra of illite, smectite, and chlorite from Welton (1984), illite and smectite apparently comprise the ridge-like morphology and chlorite forms the substrate in Figure 7A.

Chlorite was noted as a separate phase in the air-dried samples. The chlorite 002 peak was generally sharper and more prominent than the 001 peak, indicating a well-crystallized, iron-rich variety (Brindley, 1980). The high iron contents of detrital samples that contained no siderite (Tables 2 and 3) support this interpretation. One such sample (Figure 7B) contained irregular chlorite platelets and spherules having the same EDX spectrum as the substrate (EDX peak intensity: Fe < Al < Si < Mg).

The presence of chlorite made it difficult to determine whether kaolinite was present. Even-order chlorite XRD peaks coincide with the kaolinite basal 001 and 002 peaks. The 005 chlorite peak and the 003 kaolinite peak, however, can be used to differentiate

https://doi.org/10.1346/CCMN.1990.0380113 Published online by Cambridge University Press

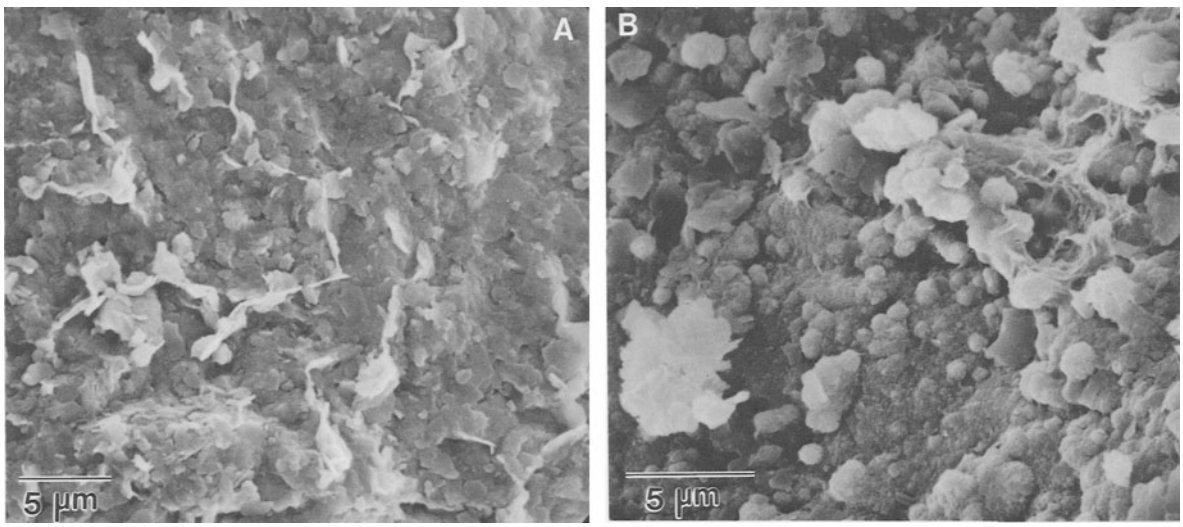

Figure 7. Scanning electron micrographs showing morphology of chlorite, illite, and smectite. (A) illite and smectite form "ridges" on a siderite(?) substrate (3000× = original magnification, sample DC 56). (B) chloritic material in sample DC 4 occurring either as platelets or rounded spherules, composed of miniscule chlorite platelets. Crenulated smectite is present in upper right part of the photo (4400×).

the two phases. The 005 peak was commonly present, but the 003 peak was not, indicating that kaolinite was probably not present or was present only in small concentrations. Scanning some samples at 2°2θ/min showed a small shoulder or peak on the low-angle side of the 004 chlorite peak, which may indicate partial resolution of a kaolinite peak. Furthermore, two 060 reflections at 1.54 and 1.49 Å were common in the XRD patterns of randomly mounted powders that contained chlorite, illite, and the expandable component, indicating that both trioctahedral and dioctahedral minerals were present.

Ten randomly selected samples containing chlorite, illite, and the expandable component were found to contain small amounts of kaolinite as evidenced by IR bands at 3694 to 3700 and 3620 cm^{-1}. Thus, many, if not most, of the detrital partings probably contained small amounts of kaolinite (Table 3).

DISCUSSION

Tephra partings

Mineral assemblages. About ⅔ of all sampled partings were apparently of volcanic origin. Based on XRD, the most common mineral assemblage of the DC section consisted of (in decreasing order of relative peak intensity) plagioclase feldspar ± (± = may or may not be present) montmorillonite ± kaolinite ± quartz ± crandallite. Clay pseudomorphs of volcanic glass were also present in many samples as determined by petrographic microscope. Illite and chlorite, which were identified in trace amounts in a few samples (e.g., samples DC 53, DC 58, and DC 70 in Table 3), probably were derived from detrital material intermixed with the tephra. The partings in the younger sections were characterized by volcanic glass ± plagioclase ± montmorillonite ± kaolinite ± quartz ± opal-CT.

Volcanic glass. Some partings in the younger sections were composed almost entirely of essentially unaltered dacitic to rhyolitic glass shards and (from XRD) traces of smectite. Assuming slow and progressive diagenesis, the absence of appreciable alteration in the younger sections may have been due to the younger age in combination with a cooler (Wolfe *et al.,* 1966) and drier (data to be reported elsewhere) climate and dry ash falls (Swineford *et al.,* 1955). The coal components (macerals) from the Sterling Formation showed some indications of a drier climate because inertinites (i.e., remnants of oxidized and/or fire-charred vegetation) were more common than in the Beluga Formation (Merritt *et al.,* 1987). Inertinites, in general, indicate a drier environment in which the swamp may have developed a desiccated surface (Stach *et al.,* 1982).

Smectite and kaolinite. Smectite was noted in nearly all tephra partings of the DC section, usually coexisting with kaolinite (Table 3). In a few samples smectite was identified without kaolinite; these partings were typically clayey bentonites. Kaolinite and smectite were probably the principal alteration products of volcanic glass and feldspar. In general, it is uncertain whether kaolinite can form directly from volcanic glass or if an intermediate montmorillonite phase is required.

Grim and Güven (1978) and Senkayi *et al.* (1984) reported kaolinite as a stable phase resulting from leaching of volcanic ash. This required a high Al:Si ratio of the ash and the removal of cations, such as Ca, Mg, Na, and K. The formation of smectite requires at

https://doi.org/10.1346/CCMN.1990.0380113 Published online by Cambridge University Press

Table 3. Representative mineralogy for crandallite, siderite-rich, detrital, and altered tephra partings as determined by X-ray powder diffraction.

Sample	K	S	I	CH	SI	C	Q	F	O
Crandallite-rich partings									
DC 1	S	T				S	S	S	
DC 8	M	M–L				T	S		
DC 12	T	M				S		M	
DC 29	L	M				T	S	S	
DC 40	S	M–L				S		T–S	
DC 40a	S	L				T		S	
DC 51	S	T				S		S	
DC 51a		T				S		M	
DC 53	S	M[1]	S	T		S		M–L	
DC 57		T				S		M–L	
DC 58	S	T[1]	S	T		T	L	S	
DC 60	T	M				S		S	
DC 60a	L					M	S		
DC 68a	L	L				S	T	L	
DC 70	L		S	S		S		M	
DC 71	M	S				S	T	M	
Siderite-rich partings									
DC 8b					M–L		S		
DC 38	K[2]	L[1]	L	M	S		L	S	
DC 48	K[2]	S[1]	S–M	S	L		S	T	
DC 56	K[3]	L	L	M–L	L		S	T?	
DC 67	S	S[1]	M	M	L		M	T	
CG 4	K[3]	L[1]	S		M–L		S	T	
Detrital partings									
DC 4	K[3]	S[1]	M–L	M			L	S	
DC 6	K[2]	S[1]	L	M			L	S	
DC 17	K[3]	T[1]	M	S			L	S	
DC 28	K[2]	T[1]	L	M			L	S	
DC 30	K[3]	T[1]	M	M			L	S	
DC 44	L	S[1]	S	S			M	M	
NIN 5	K[3]	L[1]	M–L	S			L	S	
DC altered tephra partings									
DC 8a	T	L					M	M	
DC 21	S	L					S	M–L	
DC 40d	T	M						M–L	
DC 54	S	M					S	L	
DC 65		L						L	
DC 68a	L	L					T	L	
FC, MC, NIN, CG tephra partings									
FC 6	T	L					S	T	
FC 12		S–M					S	S	
MC 3	T	S–M					T	S–M	
MC 4		L					T	S	A?
NIN 2	T	L					M	M–L	
CG 6	T	L					S	T	

K = kaolinite, S = smectite, I = illite, CH = chlorite, SI = siderite, C = crandallite, Q = quartz, F = feldspar, A = amphibole, O = other minerals that may be present in trace amounts. The approximate intensities of peaks for individual samples are noted in the different columns: L = large intensity, M = medium intensity, S = small intensity, T = trace intensity.

[1] Detected only by ethylene glycol solvation.

[2] Kaolinite present in small amounts as determined by infrared spectroscopy (IR).

[3] Kaolinite assumed to be present in small amounts based on similar samples where kaolinite was determined by infrared spectroscopy.

least partial retention of such ions (Keller, 1956). Samples from the DC section consistently contained the highest Al:Si ratios (Table 2). Thus, the smectite probably predated the kaolinite, the two clays coexisting as a result of incomplete leaching of Ca, Mg, Na, and Si.

The older DC section was probably leached over a longer period of time than the Pliocene section, resulting in more abundant kaolinite, but not over a long enough period of time for pure kaolinite to form, as have the tonsteins in the Permian and Carboniferous coal of Europe (Spears, 1970). Kaolinite formation in the DC section was also favored by a warmer (Wolfe

https://doi.org/10.1346/CCMN.1990.0380113 Published online by Cambridge University Press

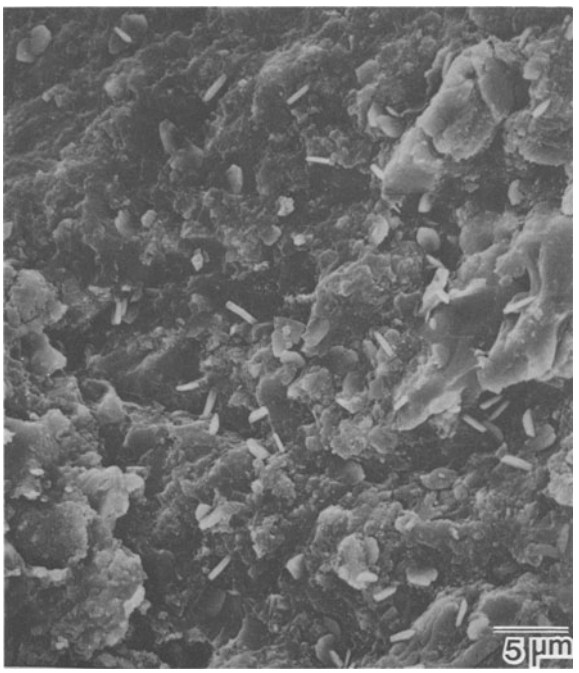

Figure 8. Scanning electron micrograph of the DC section, showing irregular kaolinite platelets on a smectitic substrate (2000× = original magnification, sample DC 37).

et al., 1966) and probably wetter (data to be reported elsewhere) climate than the younger sections. A consistent lignite to subbituminous C coal rank of the Kenai lowland coal beds (Merritt *et al.,* 1987) indicate that deep burial did not affect kaolinite formation. Igneous intrusions, that could also have affected the clay alteration have not been reported from the Kenai lowland. Based on an EDX spectrum of Al and Si, the platelets in Figure 8 are probably kaolinite. Hexagonal plates or vermiform aggregates of kaolinite were not found.

Crandallite. Crandallite-group minerals have been reported from Carboniferous (Richardson and Francis, 1971) and Cretaceous (Triplehorn and Bohor, 1983) coal-bearing sequences. In northern Alaska, crandallite minerals have been found in Cretaceous coal near Cape Lisburne, with P_2O_5 contents of 16% (D. M. Triplehorn, Department of Geology and Geophysics, University of Alaska Fairbanks, Fairbanks, Alaska 99775, personal communication, 1988). Crandallite has also been found in Chuitna River Coal Field (Rao and Smith, 1987), in the Miocene coal-bearing Tyonek Formation (Brownfield *et al.,* 1987), and in coal from Alaskan drill holes (Odum *et al.,* 1983).

Phosphate-bearing sediments in coal basins have usually been attributed to the influence of marine or brackish-water (Stach *et al.,* 1982). The coal of the Kenai lowland, however (with the exception of Hemlock Conglomerate), has been consistently interpreted as non-marine (Hayes *et al.,* 1976; Rawlinson, 1979).

Crandallite has been used as an indicator of volcanic activity and was reported to have formed early in diagenesis, before kaolinite and perhaps before or concurrently with smectite (Triplehorn and Bohor, 1983; Brownfield *et al.,* 1987). Volcanic origin of the crandallite-containing partings was indicated by Y-shaped shard (?) morphologies in Figures 5A and 9. Elongated structures in Figure 5C resembled the "columnules" described by Wise and Weaver (1979), Khoury and Eberl (1979), and Wise and Ausburn (1980). Columnules were described as diagnostic of a volcanic origin and to represent highly deformed glass shards of weld-

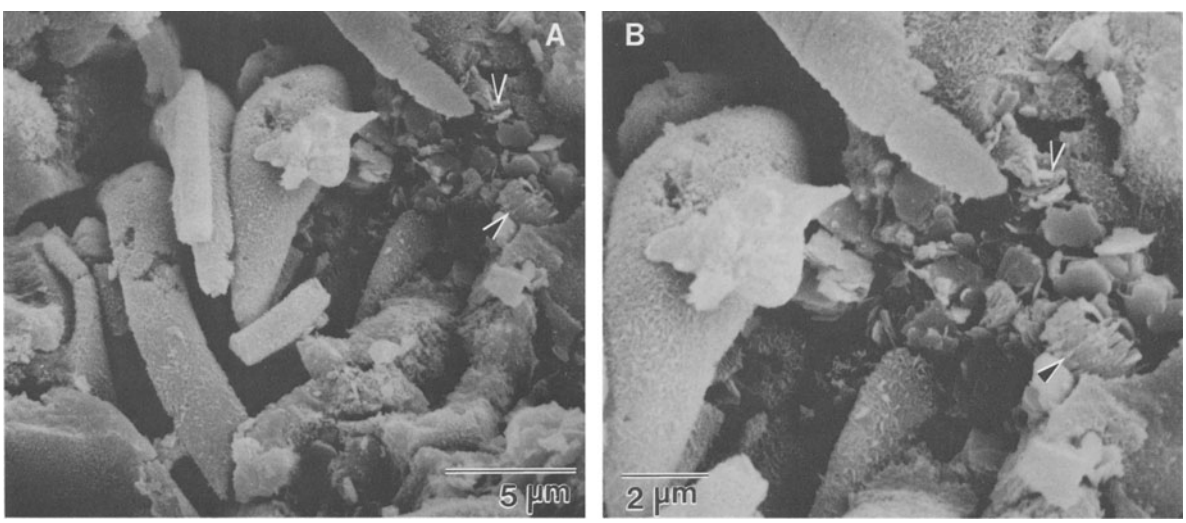

Figure 9. Scanning electron micrographs of crandallite showing shard-like morphology: (A) kaolinite appears to be replacing crandallite (arrows) in the form of irregular platelets and one rare kaolinite book. Note kaolinite apparently replacing a smooth surface, which may have collapsed from the infilling of kaolinite platelets (4400× = original magnification, sample DC 60A). (B) same photo at higher magnification (7200×).

https://doi.org/10.1346/CCMN.1990.0380113 Published online by Cambridge University Press

ed tuff that were replaced by smectite instead of crandallite. Based on EDX, a fine, crenulated crandallite layer envelopes most of the bulbous structures shown in Figures 5A–5C, indicating that volcanic bubble wall shards may have been directly replaced by crandallite. In Figure 5d, however, the crenulated material in the cavity is smectite, and the smooth surface is crandallite. In Figures 9A and 9B kaolinite appears to have replaced a crandallite-covered shard as platelets and one rare book, resulting in the shard surface losing its original shape.

Partings containing crandallite displayed no clear diagnostic macroscopic characteristics, nor did they occur in any particular position within the coal beds. Only one parting of many in a particular coal bed may contain crandallite. The only similarity between partings containing crandallite was their homogeneous fine-grained nature. This is not diagnostic, however, because many partings without crandallite also were homogeneous and fine grained. Crandallite may not have formed in the younger sections because the partings were not as altered; not because of differences in the original P_2O_5 content.

Opal-CT. Opal-CT from some partings in the younger sections may have precipitated from excess silica that was not removed from the system during dissolution of volcanic glass. This is consistent with the considerably higher whole-rock silica concentrations of these partings compared to the DC section (Table 2). Opal-CT was likely a transient phase that disappeared with silica depletion and attendant kaolinite formation.

Quartz. The lesser amount of quartz in tephra partings agrees with the observations of Senkayi *et al.* (1984, 1987). They reported that volcanic strata of the lignitic Yegua Formation contained significantly less quartz than coexisting non-volcanic layers. This relationship is also true here; either quartz was not a common component of the air-fall ejecta or some quartz dissolved. Dissolution seems less likely considering the euhedral and angular shapes of these quartz grains.

Some subrounded quartz grains in the tephra partings may be of detrital origin, from admixed wind-blown or water-deposited detritus. Larger amounts of quartz in some parts of the wide-spread Stafford Tonstein in Britain resulted from mixing of ash with normal sediments (Spears, 1970). Anomalously large amounts of quartz in individual altered tephra partings were reported by Triplehorn and Bohor (1981). Thus, characteristics such as β-quartz morphology, embayments, and straight extinction, which were found in both the DC and younger sections, are better indicators of a volcanic origin than the amount of quartz present.

Non-volcanic partings

Mineral assemblages. Based on field identification and XRD, one third of the sampled partings were apparently of detrital origin. Samples of both the DC and the younger sections typically contained chlorite + illite + smectite + quartz + feldspar ± siderite ± kaolinite. Chlorite and illite are widespread and abundant in the detrital sediments of the Cook Inlet area (Triplehorn, 1976). The clay mineral suites (<2 μm) from mudstone in the Beluga and Sterling Formations (Hayes *et al.*, 1976) generally conform with the suites of detrital partings in coal of these formations.

The reducing environment of coal swamps may have been an ideal setting for the formation of siderite. Carbon dioxide probably reacted with iron introduced by ground water, by organic complexes, or by the degradation of detrital minerals. In at least one sample, however, tephra may have been indirectly responsible for siderite formation. A 33-cm-thick, waterlain tephra parting from the CG section is gradually underlain by a siderite-bearing parting (sample CG 4). This parting contained mostly volcanic glass and small amounts of iron-bearing minerals, such as hornblende and skeletal biotite, most of which may have dissolved to provide iron for siderite formation.

In another parting (sample DC 8b), siderite occurred as nodules in a silty matrix. Blatt *et al.* (1972) suggested that concretions formed late in diagenesis tend to occupy zones of high permeability. This seems to be the case here, where siderite nodules formed as silty concretions and probably were the product of post-depositional local precipitation of siderite. Surprisingly, concretions were not more common in the sampled coal seams, because siderite concretions commonly coexist with organic compounds. Tree stumps replaced by siderite, however, were common in the coal, especially in the McNeil Canyon area.

SUMMARY

1. Volcanic ash and detrital sediments were deposited in Miocene and Pliocene coal swamps and preserved as laterally continuous layers or partings.
2. The tephra partings were generally thinner (<10 cm), coarser-grained, and more rust colored than the detrital partings. Some thin, fine-grained partings were difficult to characterize in outcrop as either volcanic or detrital.
3. Unaltered and slightly altered tephra partings were common in the younger (Pliocene) parts of the sections. Here, the tephra was mostly volcanic glass and/or montmorillonite ± opal-CT. Kaolinite was not abundant.
4. Tephra partings in the older (Miocene) parts of the section were more intensely altered. Remnant structures of pumice fragments were present. The alteration products were mainly smectite, kaolinite, and crandallite.
5. Crandallite was identified in at least 15 partings and appears to have replaced volcanic glass, before smectite and kaolinite. Y-shaped shard structures,

https://doi.org/10.1346/CCMN.1990.0380113 Published online by Cambridge University Press

hollow, bubble-wall-like shard structures, and columnules attest to a volcanic ash-fall origin.

6. The detrital partings were characterized by allogenic chlorite, illite, quartz, feldspar, authigenic siderite, and minor kaolinite and smectite.

ACKNOWLEDGMENTS

I thank M. Keskinen, D. M. Hopkins, D. M. Triplehorn, R. K. Crowder, S. A. Naidu, and T. C. Mowatt for their constructive criticism of the manuscript. R. E. Hughes, F. A. Mumpton, and A. L. Senkayi contributed with valuable suggestions to the final version of this paper. I am indebted and grateful for the support of P. D. Rao, associate director of the Mineral Industry Research Laboratory, J. E. Smith provided valuable laboratory assistance. The research for this paper, the result of which is a partial requirement for my Ph.D. degree, was funded in part by Sohio and Marathon Oil Companies and the State of Alaska.

REFERENCES

Adkison, W. L., Kelley, J. S., and Newman, K. R. (1975) Lithology and palynology of the Beluga and Sterling Formations exposed near Homer, Kenai Peninsula, Alaska: *U.S. Geol. Surv. Open-File Rept.* **75-383,** 239 pp.

Barnes, F. F. and Cobb, E. H. (1959) Geology and coal resources of the Homer district, Kenai coal field, Alaska: *U.S. Geol. Surv. Bull.* **1058-F,** 217–260.

Blatt, H., Middleton, G., and Murray, R. (1972) *Origin of Sedimentary Rocks:* 2nd ed., Prentice-Hall, Englewood Cliffs, New Jersey, 782 pp.

Brindley, G. W. (1980) Order-disorder in clay mineral structures: in *Crystal Structures of Clay Minerals and their X-ray Identification,* G. W. Brindley and G. Brown, eds., Mineralogical Society, London, 125–195.

Brownfield, M. E., Affolter, R. H., and Stricker, G. D. (1987) Crandallite group minerals in the Capps and Q coal bed, Tyonek Formation, Beluga Energy Resource Area, south-central Alaska: in *Focus on Alaska's Coal '86,* P. D. Rao, ed., *Mineral Industry Research Lab. Rept.* **72,** Fairbanks, Alaska, 142–149.

Fisher, M. A. and Magoon, L. B. (1978) Geologic framework of lower Cook Inlet, Alaska: *Amer. Assoc. Petrol. Geol. Bull.* **64,** 373–402.

Fleischer, M., Wilcox, R. E., and Matzko, J. J. (1984) Microscopic determination of the nonopaque minerals: *U.S. Geol. Surv. Bull.* **1627,** 453 pp.

Greene-Kelly, R. (1955) Dehydration of the montmorillonite minerals: *Mineral. Mag.* **30,** 604–615.

Grim, R. E. and Güven, N. (1978) *Bentonites:* Elsevier, Amsterdam, 256 pp.

Hayes, J. B., Harms, J. O., and Wilson, T. W. (1976) Contrasts between braided and meandering stream deposits, Beluga and Sterling Formations (Tertiary), Cook Inlet, Alaska: in *Recent and Ancient Environments in Alaska,* T. P. Miller, ed., *Alaska Geol. Soc. Symp. Proc.,* J1–J27.

Jackson, M. L. (1974) *Soil Chemical Analysis—Advanced Course:* 2nd ed., Published by the author, Madison, Wisconsin, 895 pp.

Keller, W. D. (1956) Clay minerals as influenced by environments of their formation: *Amer. Assoc. Petrol. Geol. Bull.* **40,** 2689–2710.

Khoury, H. N. and Eberl, D. D. (1979) Bubble-wall shards altered to montmorillonite: *Clays & Clay Minerals* **27,** 291–292.

Kinter, E. B. and Diamond, S. (1956) A new method for preparation and treatment of oriented aggregate specimens of soil clays for X-ray diffraction analysis: *Soil Science* **81,** 111–120.

Kirschner, C. E. and Lyon, C. A. (1973) Statigraphic and tectonic development of Cook Inlet petroleum province: in *Arctic Geology,* M. G. Pitcher, ed., *Amer. Assoc. Petrol. Geol. Mem.* **19,** 396–407.

Merritt, R. D., Lueck, L. L., Rawlinson, S. E., Belowich, M. A., Goff, K. M., Clough, J. G., and Reinink-Smith, L. M. (1987) Southern Kenai Peninsuala (Homer district) coal-resource assessment and mapping project: *Alaska Div. Geol. Geophys. Surv., Public-data File* **87-15,** 125 pp.

Odum, J. K., Gardner, C. A., Yehle, L. A., Schmoll, H. R., and Dearborn, L. L. (1983) Preliminary lithologic, geotechnical, and geophysical data from drill hole CW-81-2, Chuitna West coal field, Cook Inlet region, Alaska: *U.S. Geol. Surv. Open-File Rept.* **83-78,** 12 pp.

Rao, P. D. and Smith, J. E. (1987) Characterization of Chuitna Coal from deep drill core with possible applications to seam correlation: in *Focus on Alaska's Coal '86,* P. D. Rao, ed., *Mineral Industry Research Lab. Rept.* **72,** Fairbanks, Alaska, 157–182.

Rawlinson, S. E. (1979) Paleoenvironments of deposition, paleocurrent directions, and the provenance of Tertiary deposits along Kachemak Bay, Kenai Peninsula, Alaska: M.S. thesis: University of Alaska, Fairbanks, Alaska, 162 pp.

Richardson, G. and Francis, E. H. (1971) Fragmental clay (FCR) in coal-bearing sequences in Scotland and north-west England: *Proc. Yorks. Geol. Soc.* **38,** 229–260.

Senkayi, A. L., Dixon, J. B., Hossner, L. R., Abder-Ruhman, M., and Fanning, D. S. (1984) Mineralogy and genetic relationships of tonsteins, bentonite, and lignitic strata in the Eocene Yegua Formation of east-central Texas: *Clays & Clay Minerals* **32,** 259–271.

Senkayi, A. L., Ming, D. W., Dixon, J. B., and Hossner, L. R. (1987) Kaolinite, opal-CT, and clinoptilolite in altered tuffs interbedded with lignite in the Jackson Group, Texas: *Clays & Clay Minerals* **35,** 281–290.

Spears, D. A. (1970) A kaolinite mudstone (tonstein) in the British coal measures: *J. Sediment. Pet.* **35,** 610–618.

Stach, E., Mackowsky, M.-Th., Teichmüller, M., Taylor, G. H., Chandra, D., and Teichmüller, R. (1982) *Stach's Textbook of Coal Petrology:* Gebrüder Borntraeger, Berlin, 535 pp.

Swineford, A., Frye, J. C., and Leonard, A. B. (1955) Petrography of the late Tertiary ash falls in the central Great Plains: *J. Sediment. Pet.* **25,** 243–261.

Triplehorn, D. M. (1976) Volcanic ash partings in coals: Characteristics and stratigraphic significance: in *The Neogene Symposium,* A. E. Fritsch, H. TerBest, Jr., and W. W. Wornardt, eds., Papers presented at the Pacific Section, Amer. Assoc. Petrol. Geol., Soc. Econ. Paleont. Miner. Annual Meeting, San Francisco, California, 1976, 9–12.

Triplehorn, D. M. and Bohor, B. F. (1981) Altered volcanic ash partings in the C coal bed, Ferron Sandstone Member of the Mancos Shale, Emery County, Utah: *U.S. Geol. Surv. Open-File Rept.* **81-775,** 43 pp.

Triplehorn, D. M. and Bohor, B. F. (1983) Goyazite in kaolinitic altered tuff beds of Cretaceous age near Denver, Colorado: *Clays & Clay Minerals* **31,** 299–304.

Triplehorn, D. M., Turner, D. L., and Naeser, C. W. (1977) K-Ar and fission-track dating of ash partings in Tertiary coals from the Kenai Peninsula, Alaska: A radiometric age for the Homerian-Clamgulchian stage boundary: *Geol. Soc. Amer. Bull.* **88,** 1156–1160.

Van der Marel, H. W. and Beutelspacher, H. (1976) *Atlas of Infrared Spectroscopy of Clay Minerals and their Admixtures:* Elsevier, Amsterdam, 396 pp.

https://doi.org/10.1346/CCMN.1990.0380113 Published online by Cambridge University Press

Welton, J. E. (1984) *SEM Petrology Atlas:* Amer. Assoc. Petrol. Geol., Tulsa, Oklahoma, 237 pp.

Wise, S. W., Jr. and Ausburn, M. P. (1980) Kinney bentonite: Re-examined: *Scanning Electron Microscopy,* SEM Inc., AMF O'Hare, Illinois, 565–572.

Wise, S. W., Jr. and Weaver, F. M. (1979) Volcanic ash: Examples of devitrification and early diagenesis: *Scanning Electron Microscopy,* SEM Inc., AMF O'Hare, Illinois, 511–518.

Wolfe, J. A., Hopkins, D. M., and Leopold, E. B. (1966) Tertiary stratigraphy and paleobotany of the Cook Inlet region, Alaska: *U.S. Geol. Surv. Prof. Pap.* **398-A,** A1–A29.

(Received 21 June 1988; accepted 18 May 1989; Ms. 1805)

https://doi.org/10.1346/CCMN.1990.0380113 Published online by Cambridge University Press